Review

Recent progress in the study of G protein-coupled receptors with molecular dynamics computer simulations

Alan Grossfield

Department of Biochemistry and Biophysics, University of Rochester Medical Center, 601 Elmwood Ave., Box 712, Rochester, NY 14642, USA

ARTICLE INFO

ABSTRACT

G protein-coupled receptors (GPCRs) are a large, biomedically important family of proteins, and the recent explosion of new high-resolution structural information about them has provided an enormous opportunity for computational modeling to make major contributions. In particular, molecular dynamics simulations have become a driving factor in many areas of GPCR biophysics, improving our understanding of lipid–protein interaction, activation mechanisms, and internal hydration. Given that computers will continue to get faster and more structures will be solved, the importance of computational methods will only continue to grow, particularly as simulation research is more closely coupled to experiment.

© 2011 Elsevier B.V. All rights reserved.

Contents

1. Introduction

G protein-coupled receptors (GPCRs) are arguably the most important family of proteins currently studied. They are not only numerous—GPCRs are the largest family of proteins in the human genome—but exceptionally important biomedically. Indeed, it has been estimated that more than a quarter of novel drugs target GPCRs [1–3]. As a result, GPCRs have drawn an enormous amount of scientific attention, applying the entire arsenal of molecular biology, biochemistry, and biophysics. However, GPCRs, like many integral membrane proteins, are difficult to handle experimentally; they require a membrane-mimetic environment to remain folded. Thus, finding conditions to overexpress and purify them remains challenging. As a

E-mail address: alan_grossfield@urmc.rochester.edu.
URL: membrane@urmc.rochester.edu.

result, molecular level biophysical characterization of GPCR function lags behind larger-scale functional approaches, yet this detailed information will be needed to rationalize efforts in drug design and other areas of GPCR research.

In 2000, the field took a major step forward with the publication of the first high-resolution crystal structure for a GPCR, dark-state bovine rhodopsin [4]. This landmark achievement gave us the first atomic level view of GPCR structure; however, the fact remains that rhodopsin is a somewhat unusual GPCR, with a covalently bound (as opposed to diffusable) ligand, and as such it was not clear how applicable the insights from the structure would be to other GPCRs, even those in the same subfamily.

In the next few years, several new structures were solved for inactive rhodopsin [5–8], but it was not until 2007 that a second GPCR crystal structure, this time for the β_2-adrenergic receptor (B2AR), was published [9–11]. This was followed in rapid succession by two more GPCRs: the A_2A-adenosine receptor (A2A) [12] and the β_1-adrenergic receptor (B1AR) [13]. More recently, there have been a number of structures that purport to capture a more "active" form of rhodopsin, by crystallizing opsin (rhodopsin in the apo form, without its retinal ligand) with [14] or without a G protein analog bound [15], or in the presence of all-trans retinal, the agonist form of the ligand [16]. Finally, in 2010 new structures for the dopamine [17] and chemokine [18] receptors were published.

This explosion of new structural information created an opportunity for computational methods to make major contributions to our understanding of GPCR function and dynamics. The rhodopsin structures and, more recently, the structures of B2AR, B1AR, and A2A have been used as starting points for a large variety of molecular simulation projects. In this review, we will attempt to summarize the work in this field, putting the results in the broader context of GPCR function. We will not attempt a more general review of the GPCR field as a whole or even to review the impact of the X-ray structures [19–21], as this is too large a task for a single review. Moreover, we will not attempt to cover all of the computational approaches applied to GPCRs [22]; in order to control the scope of this manuscript, we will largely exclude structure prediction, ligand docking, and other related methods, in favor of a focus on more quantitative methods, primarily molecular dynamics (MD) simulations. Finally, this manuscript is not intended as an introduction to the field of GPCRs; although we will cover some of the basics, we strongly suggest beginning readers also consult the many review articles cited here. Basic GPCR behavior is also covered in most standard textbooks on molecular cell biology [23].

When referring to specific residues in GPCRs, we will use the Ballesteros–Weinstein notation; in each helix, the most conserved residue is numbered 50, and all other residues count from there [24]. Thus, the tryptophan residue involved in the rotamer toggle to activation is Trp-265 in rhodopsin, found on helix 6, would be shown as Trp-265 6.48 in a discussion of rhodopsin, or as just Trp6.48 if we were discussing the properties of that position independent of any single protein. Although including the residue number for a specific protein is not strictly part of Ballesteros–Weinstein notation, it will simplify comparisons to other papers where the notation is not used. For loops, where the residues are not well conserved, we will simply include the loop identifier, e.g., "ECL2" for extracellular loop 2.

2. Rhodopsin

Rhodopsin, the dimlight receptor in the mammalian vision system, in many ways functions as the hydrogen atom for GPCRs. It has been studied extensively, with almost 8000 papers published on it according to PubMed, starting with Wald and Clark in 1937 [25]; it was actually discovered even earlier, in the late 1800s [26]. Part of the reason rhodopsin has been so heavily studied is its ready abundance; in contrast to other GPCRs, which are typically found in very low concentrations in the cell, rhodopsin is found in high concentrations in the rod outer segment disks of the mammalian vision system. In general, it is also more tolerant of high lipid–protein ratios than other GPCRs, facilitating its study by biophysical methods, including fluorescence, infrared spectroscopy, chemical labeling, electron paramagnetic resonance, and solid state NMR [27]. This also facilitated the protein's crystallization and led to the first high-resolution GPCR structures in 2000 [4–8,28].

As a direct result, rhodopsin has also been heavily studied using MD simulations, far more so than the other GPCRs. In particular, a significant amount of work has focused on the role of lipid–protein interactions in modulating rhodopsin function, including the possible functional role of oligomers, and on the conformational changes undergone during the activation process.

2.1. Lipid–protein interactions in the dark state

2.1.1. Polyunsaturated ω-3 lipids

The environment surrounding a biomolecule is critical to its behavior, stabilizing the formation of a native state and modulating the fluctuations that drive function. For membrane proteins, this manifests in the ways that the lipid composition of a bilayer alters the stability and efficiency proteins embedded in it [29–33].

Rhodopsin is a particularly interesting example of this phenomenon. Its native environment, the rod outer segment (ROS) membranes of rod cells of the mammalian vision system, have very unusual lipid compositions. First, they are highly enriched in polyunsaturated ω-3 fatty acids [34]; given that natural lipids nearly always have a saturated fatty acid in the sn-1 position, the results suggest that most lipids have a polyunsaturated chain. This is remarkable considering that mammals cannot synthesize ω-3 fatty acids themselves, and the overall abundance of ω-3s at the organism level is more likely 5%. Second, the cholesterol concentration is quite high in ROS membranes but is not uniform [34]. Rather, it is very high in immature ROS disks and gradually drops as the disks migrate toward the top of the stack. This clearly indicates that the cell is carefully controlling the ROS membranes' lipid composition, and since almost all of the protein in those membranes is rhodopsin it is unsurprising that experimental work in vitro shows that both ω-3s and cholesterol have significant effects on rhodopsin's activity. In particular, polyunsaturated lipids enhance rhodopsin function, pushing the Meta-I/Meta-II equilibrium toward the active Meta-II state [35], while cholesterol has the opposite effect [36].

Given that both cholesterol and ω-3s alter the bulk properties of liquid crystalline membranes—cholesterol increases order while ω-3s are highly disordered [37], it would be interesting to know the mechanism by which they each modulate rhodopsin. Specifically, do they form specific interactions with the protein, or is their effect due just to their effects on membrane elasticity or other bulk properties?

For the polyunsaturated lipids, the first evidence from simulations came from a molecular dynamics simulation of rhodopsin in a 1-stearoyl-2-docosahexaenoyl phosphatidylcholine (SDPC) membrane by Feller et al. [38]. Although the simulations were relatively short (12.5 ns), there was a clear preference for the ω-3 docosahexanoyl chains to interact with the protein, with a concomitant exclusion of the saturated stearoyl chains.

Grossfield and coworkers followed this up by considering the dynamics of rhodopsin in a realistic membrane composition containing SDPC, SDPE (phosphatidylethanolamine), and cholesterol [39,40]. The presence of multiple lipid species meant that lateral reorganization of the membrane, which occurs on the microsecond scale or slower, had to be taken into account. Accordingly, they chose to perform 26 separate 100 ns simulations (as opposed to a single long trajectory), rebuilding the bilayer from scratch each time to ensure that a number of truly independent bilayer conformations were explored. The results were consistent with those seen previously [38];

the density of the ω-3 chains at the protein surface was clearly enhanced but the improvement in sampling allowed more detailed analysis. In particular, the paper identified eight distinct sites on the protein surface that repeatedly formed tight interactions with docosahexaenoyl chains, consistent with solid state NMR results suggesting specific binding [40,41]. Later analysis of the statistics of chain states suggested that the preference for polyunsaturated chains at the protein surface was entropically driven, in that the ω-3 chains experience a far lower entropic penalty than saturated chains when partitioning to the protein surface [42]. A smaller number of less populated clusters were identified for stearoyl chains and cholesterol. Although previous simulation work suggested that cholesterol is largely excluded from the protein surface [39,40], a more recent 1.6 μs simulation of rhodopsin suggested that cholesterol–protein interactions may modulate the kink angles of helix 7 [43].

There is also significant evidence that the headgroup composition can also affect rhodopsin function, and that in particular PE headgroups enhance rhodopsin function [44,45]. However, the time scale of lateral reorganization appears too long for this to be directly addressed by all-atom simulations at this time [40].

2.1.2. Oligomerization

Over the last few years, the role of oligomerization in GPCR function has been intensely debated [46]. On one hand, there is significant experimental evidence for homo- and hetero-dimerization under some conditions [47–53]. Similarly, computational work from Filizola and coworkers has argued that rhodopsin forms dimers [54] and that other GPCRs form heterodimers [55]. Along the same lines, coarse-grained (CG) molecular dynamics simulations of rhodopsin in a series of lipid bilayers with varying hydrophobic thicknesses clearly demonstrated the role of lipid–protein interactions in modulating oligomerization [56].

On the other hand, the nature of the physiologically relevant state is less clear, particularly since the nature of the lipid environment can easily change the thermodynamic balance between monomer and dimer [57]. Early evidence suggested that rhodopsin functions as a monomer [50,58,59], and more recent calorimetry experiments indicate that in its native ROS membranes, rhodopsin is primarily monomeric [60]. Furthermore, rhodopsin is capable of binding G protein in its monomeric form [61–66].

As a result, the simulation community faces a significant degree of ambiguity: what state should we simulate? The vast majority of simulations of GPCRs have considered only the monomeric form, but is this a good model for the in vivo behavior? This is a case where there arguably is no ideal choice, at least given the present state of knowledge. On one hand, we want to simulate the conditions that best resemble those found experimentally in vitro and in vivo, which might argue in favor of modeling dimers. However, modeling dimers brings with it a number of major technical challenges. To start with, the simulation system would need to be much larger, greatly increasing the computational cost and significantly reducing the length of the trajectory that can be run. At the same time, the protein system is larger, and thus will have slower fluctuation modes that need to be sampled, meaning that a longer trajectory would be required to acquire equivalent statistical sampling. Generating good statistics is already a significant problem even for monomeric systems; although many of the longest all-atom trajectories ever run have been simulations of GPCRs [40,67–71], careful analysis of the convergence has shown that the microsecond-scale is almost certainly not long enough to draw firm conclusions about many of the most interesting phenomena [72–74]; this will be discussed more extensively in Section 5.

The final and perhaps most important challenge is due to the simple fact that we do not know exactly what dimer (or higher-order oligomer) to use. Although a number of researchers have constructed models of dimers (for one example, see the work of Filizola, Weinstein and coworkers [54,55,75–77] and others [78]), the fact remains there is no crystal structure of a biologically relevant dimer, and the overall record of homology modeling and related efforts does not give us high confidence in the atomic level accuracy of such models. Thus, even if the overall orientations of the monomers in the dimer are correctly predicted, it is almost certain that many smaller-level details are not. This in turn means that we must rely on the simulations to fix the problems for us, something not guaranteed to happen over the course of a typical MD simulation. Indeed, the largest concern is that there would be no real way to know if the starting structure was badly flawed: one could easily imagine a mis-packed dimer persisting for hundreds of nanoseconds or longer.

Perhaps the only exception to this concern is the judicious use of coarse-graining, which would extend the simulated time scales enough to allow dimers to spontaneously form and dissociate under equilibrium conditions. Indeed, Periole et al. used precisely this approach very successfully [56]; each of their CG simulations contained 16 rhodopsin molecules, and they systematically examined the effect on oligomerization of varying the bilayer thickness. Although their primary conclusion—hydrophobic mismatch greatly increases the propensity of rhodopsin to oligomerize—is not an enormous surprise, their work is an excellent example of the potential for simulations to vividly illustrate biophysical principles. While their model contains some very significant approximations, including a large number of restraints needed to keep the proteins near the native state, it is wholly appropriate for the context in which it is used.

2.2. Investigations of the activation mechanism

One of the key questions in the rhodopsin field (and the GPCR field in general) is the nature of the conformational changes that occur during activation. The common model [23] of GPCR–G protein function is that ligand binding from the extracellular face (or ligand isomerization in the case of rhodopsin and retinal) drives a series of conformational changes that propagate to the intracellular loops, allowing the G protein trimer to bind and exchange GDP for GTP. As a result, the G protein trimer dissociates into Gα and Gβγ subunits, which in turn continue the signaling cascade by changing the behavior of other proteins, for example adenylate cyclase.

Rhodopsin's structural changes during activation have been studied extensively using a variety of techniques, including cysteine scanning, EPR, NMR, and of course crystallography [27,79]. However, there has been no crystal structure of a truly "active" GPCR, in part because assessing activity in the context of a crystal is exceptionally challenging, as it would arguably require crystallizing the full GPCR–G protein complex. The closest examples to date are the crystal structures of opsin on its own [14] and with a G protein fragment bound [15].

As a result, the idea of using MD simulations to directly explore the activation mechanism is highly attractive, and efforts began shortly after publication of the original rhodopsin crystal structure. Schulten and co-workers published a 10 ns MD simulation of rhodopsin in a 1-palmitoyl-2-oleoyl phosphatidylcholine (POPC) membrane, focusing primarily on the retinal conformation and the relaxation of the side chains in the binding pocket [80]. Unsurprisingly, they did not see isomerization of Trp-2656.48, because the expected timescale for that motion is significantly longer. However, they did observe significant relocation of the retinal β-ionone ring, consistent with experimental cross-linking data from Borhan et al. [81].

Lemaˆıtre et al. also explored the relaxation of the retinal post-isomerization [82]. They performed a 10 ns dark-state simulation as equilibration, then used steered MD to flip the retinal torsion to the trans state. They performed this flipping three independent times, and continued each simulation using conventional molecular dynamics for 10 ns. The analysis focused on the details of the retinal conformation, with careful comparison to solid state NMR experiments from the same group. Although the calculations are very short

by current standards, the paper is noteworthy for its use of multiple trajectories: running three separate trajectories allowed the authors to attempt to assess which of the conformational changes upon retinal isomerization are critical parts of the activation mechanism.

Crozier et al. published a far more extensive simulation a few years later [83]; by running for 150 ns (as opposed to 10 ns), they were able to see more of the protein's response to retinal isomerization. As in the earlier work by Saam et al. [80], they observed that the ionone ring approached Ala-169[4.58], consistent with chemical cross-linking data [81]; indeed, because the simulations were an order of magnitude longer, they saw far more extensive motion in this regard, with the final separation between moieties around 9 Å. They also observed a number of changes in helical tilts and kink angles, although in the absence of a comparable dark-state simulation it is difficult to know how much of these changes is due to retinal isomerization. Additionally, they saw the salt bridge break between Glu-113[3.28] and the protonated Schiff base linking retinal to Lys-296[7.43], as expected during activation; see Section 2.2.1 for more discussion of the salt bridge behavior.

Recently, Hornak et al. published a very interesting paper where they used experimentally determined distance changes as energetic restraints; applying these restraints in a simulation efficiently drove rhodopsin toward the active Meta-II state [84]. Essentially, they used magic angle spinning NMR to measure a set of interatomic distances in the Meta-II state, primarily between carbons in the retinal and the surrounding residues, and selected those that differed significantly from the crystal structure (PDB code 1U19). The selected distances were used as additional restraints in a MD simulation of rhodopsin in a bilayer-mimetic environment, in effect forcing it to become consistent with the distances measured in the Meta-II state. This allowed them to observe activation-like motions in very short simulations, typically only a few ns in duration. In particular, they observed significant motion by helix 6, including disruption of the ionic lock, and displacement of extracellular loop 2 (EL2), which forms the "lid" enclosing the retinal binding pocket.

Although the method is very clever and the results largely persuasive, there is a significant reservation when interpreting this kind of result, one common to most steered MD-type applications: although the end points are reasonably well-determined, the path taken during the trajectory is not guaranteed to be physiologically relevant. In the cell, rhodopsin proceeds from dark state to Meta-I on the microsecond scale, which then interconverts with Meta-II on the millisecond scale (although much of this delay may be due to waiting for the retinal Schiff base linkage to deprotonate, a necessary step for Meta-II formation). Here, while we can be confident that the restrained residues end up in conformations consistent with experiment (and there are enough redundancies to strongly suggest that the overall binding pocket changes are probably correct), it is not clear that the remainder of the protein has "caught up." That is, those portions of the protein that are not altered by the experimental restraints are rapidly perturbed by their application, and the trajectories may not be long enough for them to relax, let alone fully sample their equilibrium distributions. This is a major concern, given that previous work has demonstrated that simulations two orders of magnitude longer do not effectively converge the motions of individual loops [72], let alone the protein as a whole (see Section 5 for further discussion).

2.2.1. Salt bridge to protonated Schiff base

In all of the rhodopsin crystal structures, the salt bridge between Glu-113[3.28] and the protonated Schiff base linkage between Lys-296[7.43] and the retinal is easily observed. Moreover, it is well known that this interaction is at least partially disrupted during protein activation. However, the exact mechanism by which this occurs has been the subject of significant controversy. Two competing models exist for the role of two internal glutamates (Glu-113[3.28] and Glu-
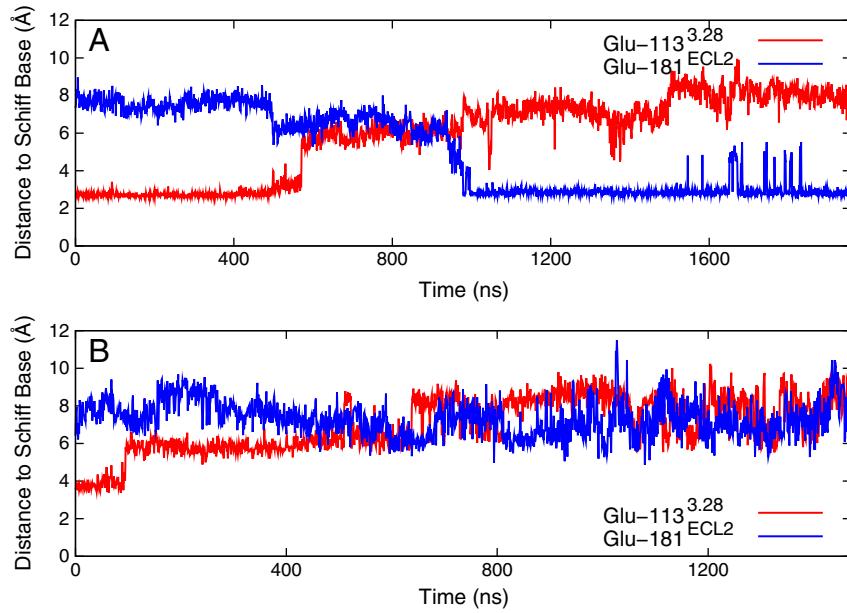
181ECL2). One model, commonly referred to as the counterion switch model [85], argues that the latter glutamate is protonated in dark-state rhodopsin. After retinal isomerization, this proton is transferred to Glu-113[3.28], causing the salt bridge to break. After some reorganization, the Schiff base forms a salt bridge to Glu-181[ECL2], signaling formation of the Meta-I state. By contrast, the complex counterion model of Lüdeke et al. [86] argues that both glutamates are deprotonated throughout the process and that upon retinal isomerization the Schiff base is effectively "shared" by the two glutamates.

Röhrig, Rothlisberger and coworkers looked extensively at this issue, systematically using Poisson–Boltzmann methods, classical molecular dynamics, and mixed quantum/classical calculations [87,88]. Their results were most consistent with the complex counterion model, although the trajectories (particularly the QM-MM ones) are fairly short. More recently, Röhrig and Sebastiani compared computed chemical shifts from a QM-MM trajectory to experiments, but were unable to definitively determine which model is more likely [89].

Recent advances in supercomputer technology have allowed enormous increases in the scale of classical molecular dynamics simulations [90,91]. Grossfield and coworkers took advantage of these gains to test both mechanisms directly, using classical MD methods [67,92]. They performed two separate all-atom simulations of the activation process. In the first, designed to test the counterion switch model, they began with an equilibrated model with Glu-181ECL2 protonated [39]; they induced the retinal torsion to flip from cis to trans and ran for 500 ns. They then stopped the simulation, manually moved the proton from Glu-181ECL2 to Glu-113.28, and continued the simulation for an additional 1500 ns. To test the complex counterion model, they similarly generated an equilibrated structure with both glutamates in the charged state [40], flipped the retinal torsion, and ran for an additional 1500 ns. At the time of publication, each of these simulations was longer than any previously published all-atom trajectory of a membrane protein (or any other comparably sized system).

These results indicated that both trajectories behaved essentially the way their underlying models suggested they should. In particular, Grossfield et al. tracked the distances between the glutamate carbonyl oxygens and the Schiff base nitrogen in both trajectories, as seen in Fig. 1 [67]. In Part A, showing the counterion shift trajectory, the Glu-113.28–Schiff base salt bridge remains stable until the 500 ns point, where the proton was moved to Glu-181ECL2. The interaction then quickly breaks and, a few hundred nanoseconds later, is replaced by a salt bridge to the now-charged Glu-181[ECL2]. In Part B, the complex counterion trajectory, the salt bridge breaks after about 100 ns, and the Schiff base gradually approaches Glu-181[ECL2], although both glutamates make strong interactions with it.

On one hand, these calculations strongly suggest that both models approached something like the Meta-I state; in each case, the glutamates did precisely what the underlying models said they should. On the other, there is not enough information to determine which of the two models is more likely correct. To do so, Martínez-Mayorga et al. compared the trajectories to solid state NMR results [92]. Brown and coworkers previously reconstituted rhodopsin with retinal specifically deuterated at particular methyl groups. From the deuterium spectra, they predicted the orientation of the ionone ring in the dark state and Meta-I [93,94] by finding the single conformation that produced a theoretical line shape [95] most consistent with the experimental spectrum. Martínez-Mayorga et al. in a sense reversed this approach, computing theoretical NMR spectra from the MD trajectories by generating histograms of the methyl group orientations and using them to compute a weighted average spectrum. As shown in Fig. 2, one trajectory—the complex counterion—produced extremely accurate results, while the counterion switch trajectory produced spectra that differ substantially from experiment,
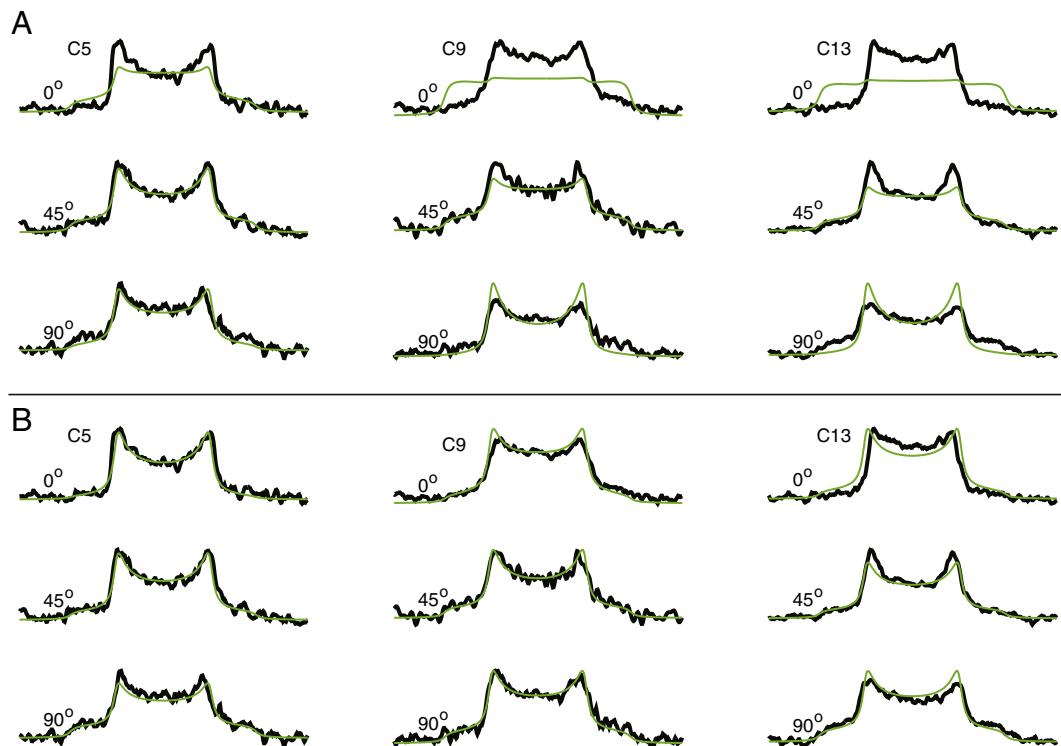
Fig. 1. Distance between internal glutamates and the Schiff base during simulations of rhodopsin activation. Part A shows the distances in the counterion switch simulation, while Part B shows the complex counterion trajectory. The results were previously published in reference [67].

particularly at 0° tilt. Interestingly, when the same approach was applied to an ensemble of dark-state rhodopsin trajectories, the results revealed that the ionone ring assumes two distinct orientations in the dark state [96]; the spectra computed from the full ensemble matched the experiment significantly better than did the subset of the ensemble where the ionone assumed the orientation found in the crystal structure (see Figs. 1d and 4 from reference [96]). These results underscore the power of close collaboration between simulation and experimental groups, and in particular the critical importance of directly computing the experimental observable, rather than simply comparing to the interpretation of the experimental results.

2.2.2. Internal hydration changes upon activation

A protein's interactions with water are critical to its structure, dynamics, and function, and the hydrophobic effect is one of the key

Fig. 2. Comparison between theoretical and experimental deuterium spectra. The black lines show experimental deuterium NMR spectra for the C5, C9, and C13 methyl groups of retinal, with samples oriented at 0°, 45°, and 90° relative to the magnetic field. The green curves show equivalent theoretical spectra computed from the distribution of angles found in the simulations. Part A shows the results for the couterion switch simulation, and Part B shows the results for the complex counterion simulation. These results were previously published in reference [92].
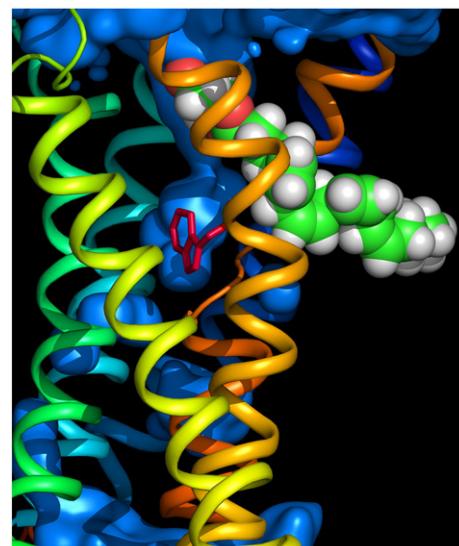
drivers of protein folding. Despite this, it is not immediately obvious that changes in the hydration of an already folded protein should play a functional role, particularly for integral membrane proteins. However, there is significant experimental evidence that internal hydration is important for the function of rhodopsin and perhaps other GPCRs as well. For example, Mitchell, Litman, and coworkers established that the presence of alcohols, sugars, and other osmolytes in the surrounding medium significantly alters the equilibrium between the Meta-I and Meta-II states of rhodopsin [98–101], suggesting that the active Meta-II state is less hydrated than Meta-I. Moreover, the higher-resolution GPCR crystal structures all contain numerous internal water molecules in functionally relevant locations [5,102–105].

Still, it was a significant surprise when Grossfield et al. argued that the internal hydration of rhodopsin increases dramatically during the transition from the dark state to Meta-I [67]. In a 1500 ns simulation modeling the complex counterion model of activation, they observed the number of waters inside the protein increasing from 15–20 to around 60; the exact number is sensitive to the criterion for what constitutes the "inside" of the protein, but the trend is unmistakable. Critically, they performed a dark-state simulation of comparable length, where the hydration remained steady, precluding the objection that the hydration changes were a failure of the simulation, due to poor construction or flaws in the force field. The same paper also contained a novel experimental confirmation, via magic angle spinning (MAS) ^{1}H NMR. They saturated the water resonances and observed attenuation of lipid hydrocarbon resonances, suggesting magnetization transfer between water and lipid. However, the effect was absent in lipid systems without rhodopsin, and was significantly stronger in the Meta-I state than in the dark or Meta-II states, confirming that the magnetization transfer is protein-mediated, via long-lived protein–water interactions. The lifetime of waters inside the protein cavity was typically on the timescale of 1–10 ns, although a few water remained inside longer; this contrasts sharply with more recent experiments suggesting residence times of seconds or longer [103–105].

The simulation result was surprising enough to lack credibility on its own, particularly given the unprecedented (at the time) length of the trajectories; in the absence of experimental confirmation, it would likely have been dismissed. However, it challenged their experimental collaborators to more carefully examine their experimental results on attenuation of lipid signals with presaturation of proton resonances of proteins, lipid, and water at various frequencies. This led to the discovery that presaturation of the water resonance led to lipid resonance attenuation that depended on rhodopsin's state [106]. It was only when the simulations and experiments were combined that credible interpretation became possible.

These results raise the question of generality: is this hydration behavior unique to bovine rhodopsin–rhodopsin is after all an unusual GPCR, or is it a general property of GPCRs in general? A recent simulation of squid rhodopsin carefully analyzed the dynamics of internal water molecules, and implicated these waters in the activation mechanism [107], although the overall hydration levels were much lower than in the above calculations, and the trajectory was too short to see any activation-like fluctuations.
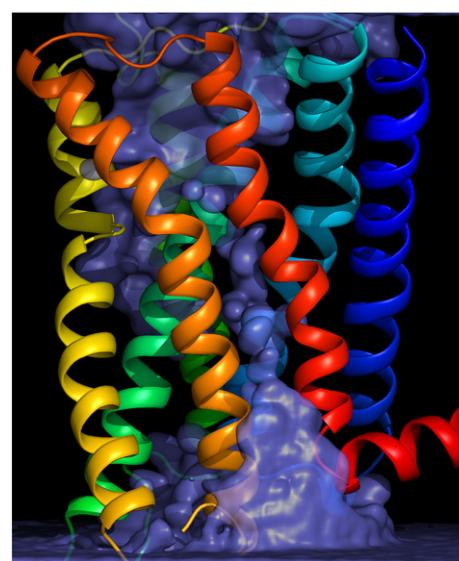
Similar behavior was also seen in simulations of other, non-rhodopsin, GPCRs. For example, microsecond-scale simulations of the cannabinoid 2 (CB2) receptor by Hurst et al. also showed hydration increases [97]; these calculations showed the spontaneous binding of CB2's native ligand, 2-arachidonylglycerol (2AG), from the membrane medium. Because CB2 needs to change protonation states as part of its activation mechanism, the authors then "manually" protonated Asp-130$^{3.49}$ and Asp-240$^{6.30}$, then continued the simulation for an additional 2 µs. As shown in Fig. 3, the combination of 2AG binding and sidechain protonation led to a series of activation-like events, including repacking and partial disassembly of the interface between


Fig. 3. Spontaneous ligand binding and subsequent activation-like structural changes in the CB2 cannabinoid-2 receptor. The protein is shown as a ribbon model with the intracellular face at the bottom, the 2AG ligand molecule is shown in a space-filling view, and Trp-258$^{6.48}$ is shown in red. Water oxygens within 15 Å of the protein principal axis were histogrammed in 0.25 Å^3 bins, smoothed with a 2 Å gaussian and shown as blue surfaces contoured at half of bulk density. Data were originally published in reference [97].

helices 3 and 6 (where the ionic lock is usually found) and isomerization of Trp-258$^{6.48}$. This in turn opens a continuous water channel connecting the intracellular and extracellular domains via the ligand binding pocket, allowing a dramatic increase in internal hydration.

Furthermore, two simulations of B2AR also discussed the role of internal hydration [68,108]; Fig. 4 is a visualization of the average water density over the course of one of these trajectories [68]. The water density is contoured at half of bulk density, showing that there are several regions inside the protein that are perpetually hydrated. In particular, the ligand binding pocket (the protein was simulated in the apo form) filled with water during the equilibration period and

**Fig. 4.** Internal hydration of B2AR from molecular dynamics simulation. The average protein structure from the simulation is shown in ribbon format. Water molecules were histogrammed on a 0.25 Å3 grid, smoothed via convolution with a 2 Å gaussian, and contoured at half of bulk density. Only waters within 15 Å of the protein principle axis are shown. The underlying data was previously published in reference [68].

remained hydrated throughout the trajectory. Water also played a central role in the "ionic lock" region, a highly conserved salt bridge between Arg-1313.50 and Glu-2686.30 that breaks upon activation; the simulation showed that the ionic lock frequently exists in a water-bridged form, as opposed to a simple salt bridge. More recently, Kaszuba et al. argued that water-ligand interactions in the B2AR binding pocket contribute significantly to B2AR selectivity for closely related ligands [108], consistent with other analyses showing that internal hydration strongly modulates ligand binding [109].

Overall, the preponderance of evidence indicates that GPCR hydration is probably central to their functional fluctuations; we believe this will be a fruitful area for future study by both computational and experimental means.

3. Simulations of GPCR–G protein interactions

The next critical stage in the molecular simulation of GPCRs is to attack the full activation mechanism: the interaction with G protein and subsequent dissociation of the trimer. Although going after this problem computationally is attractive and could potentially yield a wealth of functionally relevant information, this is an exceptionally challenging problem. First, there is no high-resolution experimental data describing the structure of the full complex, and the complex of an integral membrane protein with a relatively large (trimeric) soluble protein is a difficult target for crystallography. Moreover, if we assume that the dogma in the GPCR field is correct and specific G protein association only occurs when the GPCR is in its active state, even the GPCR structure is not well known; this severely complicates efforts to use docking and homology modeling techniques to generate a starting structure. Second, the resulting complex is extremely large by current molecular dynamics standards (particularly once sufficient water to hydrate the G protein is included), which dramatically increases both the computational cost per nanosecond of trajectory time and the length of trajectory needed for statistically significant sampling of the relevant fluctuations.

Despite these challenges, a few groups have attempted calculations involving the full GPCR–G protein complex. Raimondi et al. used a combination of homology modeling, docking, and molecular dynamics to examine the thromboxane A_2 receptor bound to its cognate G protein [110]. Although the paper is very ambitious, there are some serious concerns in interpreting their results. First, as discussed above, there is significant uncertainty in their starting structure, particularly since there is no crystal structure for the GPCR. Second, the MD simulations themselves are extremely short, less than 10 ns, shorter than the correlation time for sampling protein structures even in the case where no relaxation of the starting structure is required. This is particularly concerning given their reliance on essential dynamics methods in their analysis, because the slow modes converge very slowly in GPCRs [72–74].

Last year, Sgourakis and Garcia published a calculation of truly remarkable scope: an all-atom MD simulation of the rhodopsin–transducin complex in an explicit lipid bilayer [111]. To our knowledge, this represents the largest computational investment ever made in a single calculation, a 400,000 atom system run for over 1 μs. The system is an attempt to model the interaction between dark-state rhodopsin and its G protein partner, transducin, in the GDP-bound state. This is an impressive attempt to attack an exceptionally difficult problem, one which reveals both the challenges and opportunities involved with such calculations. For example, the calculations revealed the dynamic nature of the interactions between rhodopsin and the G protein α subunit, and explored the details of intra- and inter-molecular salt bridge dynamics.

However, the simulation was not started from a crystal structure, but rather a docking model [112,113]. This would be less of a concern were the existence of the putative complex not so controversial; although there is some evidence that rhodopsin can form specific interactions with G proteins even with retinal in the inactivating 11-cis conformation, this runs counter to the current dogma in the field. Furthermore, the interface between the two proteins repacks over the course of the trajectory, forming a significantly looser set of contacts (see Fig. 2 of reference [111]). This could be interpreted to mean that the complex is dynamic and samples a broad range of structures. However, it could also mean that there are flaws in the starting structure. Unfortunately there is no obvious way to tell which of these hypotheses is correct; proving the former case would likely require a simulation 1 to 2 orders of magnitude longer. Given that the present work is already heroic by current standards, this underlies the challenges of performing all-atom calculations.

4. Simulations of other GPCRs

Although the GPCR MD literature emphasizes rhodopsin for obvious historical reasons, the more recently published GPCR structures have also been simulated extensively [68–70,108,114, 115] To our knowledge, the first large-scale all-atom simulation of B2AR, the second GPCR crystallized and solved, was published by Huber et al. [114]; this very valuable paper is written as much as a review of the implications of the new crystal structure as it is an analysis of simulation. They chose to simulate the full chimeric protein from the crystal—B2AR with T4 lysozyme inserted between helices 5 and 6 [9,10], in the presence of the inverse agonist ligand, carazolol; they also performed simulations of the physiological ligand, adrenaline. Interestingly, they mention that the internal hydration of the protein increases in the adrenaline simulation, consistent with the rhodopsin results discussed in Section 2.2.2.

The following year, Vanni et al. published a series of simulations comparing the dynamics of B2AR and B1AR, focusing on the dynamics of the ionic lock [115]. The ionic lock is a highly conserved salt bridge between $Arg^{3.50}$ and $Glu^{6.30}$ thought to be crucial to maintaining the inactive form of class A GPCRs; mutations to these residues tend lead to constitutively active proteins [116,117]. As a result, the community at large was surprised when the crystal structures of B2AR, B1AR, and A2A all lacked this salt bridge. In the case of B2AR, the ionic bond is displaced by a salt bridge to a symmetry-related T4 lysozyme molecule, and more generally the accepted hypothesis is that the modifications needed to induce the GPCRs to crystallize—the presence of the antibody or fusion protein—altered the conformational equilibrium in this region. Accordingly, it was very welcome to see the careful analysis of the salt bridge in the Vanni et al. manuscript [115]. They argue that the salt bridge's state depends on the protonation state of another highly conserved residue, $Asp^{2.50}$, even though this residue is roughly 20 Å away; in their calculations, the salt bridge is only stable when the aspartic acid residue is protonated.

Dror et al. performed a series of very long simulations of B2AR (five ≈ 1 μs, another over 2 μs), also focusing on the ionic lock [69]. They examined the role of the third intracellular loop (ICL3), performing simulations with it clipped out, replaced with a model-built version of the native loop, and with the full T4 lysozyme as seen in the crystal structure. They found that ionic lock generally formed stably in the clipped and native simulations, but the presence of the lysozyme significantly destabilized it. Moreover, when they simulated a pair of constitutively active mutants with disrupted ionic locks, they found that the helices in question (3 and 6) moved apart somewhat, consistent with consensus models for activation.

The analysis of B2AR's internal hydration from Romo et al. (another microsecond-scale simulation) [68] were discussed above in Section 2.2.2. However, that work too discussed the state of the ionic lock; they found that the lock existed in three distinct states: closed, open, and water-bridged (where the two side chains each formed hydrogen bonds to the same water molecule), and that the three states rapidly inter-convert, on the nanosecond time scale. In this simulation, the authors observed a single "activation-like" event,

where the intracellular end of helix 6 tightened into a 3–10 helix, moving the sidechain of Glu-268[6.30] far from its salt bridge partner. Roughly 200 ns later, the helix returned to a more conventional α-helical state, and the salt bridge resumed its previous noisy association.

Finally, Lyman et al. conducted what is to our knowledge the only large-scale simulation study of A2A [71]. They compared the binding pocket fluctuations of the protein with an antagonist bound to those in the apo state, and found significant conformational rearrangement when the antagonist was removed, including isomerization of the rotamer toggle (Trp-246[6.48]). However, the apo form of the protein is significantly stabilized by binding a cholesterol molecule between helices 1, 2, 3, and 4; the equivalent region of rhodopsin was predicted to bind cholesterol in previous simulations [40].

5. Assessing statistical errors in simulations

There are two key questions one must ask of every molecular dynamics paper in order to evaluate its questions: (1) Is the model appropriate for the scientific question? (2) Are the statistics good enough to draw conclusions? The first question includes issues of force field quality (including the potential need for polarizable force fields or even quantum mechanical models), system size and composition, etc. While these issues are important, they have been reviewed elsewhere numerous times, and in any event they are not uniquely important in the study of GPCRs [118]. Indeed, as Zuckerman and coworkers point out, it is often impossible to assess whether new models are actually improvements without good sampling [119]. Moreover, many (perhaps most) of the longest all-atom molecular dynamics trajectories performed in recent years have involved GPCRs [40,42,43,67–69,92,120], and as a result they have been used as test cases for sampling and convergence [72,73,119].

There are a number of ways of framing the problem of statistical sampling: How do you compute error bars for quantities of interest? How many independent samples does the simulation provide? What are the relevant relaxation times for the system?

In some sense, these questions are tightly related: the correlation times for the system (combined with the trajectory length) determine the number of truly independent data points in the system, and the statistics for independent, uncorrelated data sets are relatively simple. In that case, the statistical uncertainty for a quantity A is well estimated by the standard error

$$SE(A) = \frac{\sigma(A)}{\sqrt{N_{ind}}} \approx \sigma(A)\sqrt{\frac{\tau(A)}{T_{sim}}} \tag{1}$$

where SE is the standard error, σ is the standard deviation, N_{ind} is the number of independent samples, T is the correlation time, and T_{sim} is the length of the simulation [73]. However, the challenge remains in determining what N_{ind} actually is.

When trying to assess the statistical uncertainty of a single scalar quantity, the standard approach is block averaging [121]. In this approach, the full trajectory is divided in M blocks, and the average value for the quantity of interest (A) is computed for each block. The blocked standard error is then

$$SE_M(A) = \frac{\sigma_M(A)}{\sqrt{M}}. \tag{2}$$

The true standard error for the full trajectory is estimated as the limiting value as the individual blocks become long and thus statistically independent. Although this method is simple to implement, there are certain difficulties in its use. First, as the length of the individual blocks gets longer, the number of blocks necessarily decreases, and as a result the standard error plot can get very noisy. To some extent, if the noise is large enough that one cannot read off a

standard error (or even determine if a plateau has been reached), this should serve as an indicator that the simulation is far too short. However, at the very least the need to determine a plateau complicates the use of the block averaged standard error in an automated way. Second, block averaging does not directly yield a correlation time, and although one can estimate it using Eq. (1), this estimate is typically low by perhaps a factor of 2 [73,122]. Third, if the quantity of interest, A, is coupled to some other, far slower, quantity B, it may not be immediately obvious from just the time series of A [73]. It should be noted that the term "block averaging" is often misused in the literature to mean a standard deviation or standard error computed from a single fixed number of blocks, without any verification that this number of blocks is from the plateau region of the SE_M curve.

As a result, it is desirable to find a better way to assess statistical convergence, one which directly examines the largest scale (and likely slowest) relevant modes in the system of interest. It is important to include the term "relevant" in the previous sentence, because there are always slower modes that will not be captured in a simulation that do not contribute significantly to ensemble averages, for example spontaneous protein unfolding under native conditions.

One interesting piece of work focusing on the convergence of membrane proteins came from Faraĺdo-Gomez et al., who tried to assess convergence by comparing two halves of 10 ns trajectories of a number of proteins, including rhodopsin [123]. Among their innovations was their application of principal component analysis, quantitatively comparing the fluctuation spaces using a quantity called the covariance overlap (originally developed by Hess [124,125]):

$$\Omega_{AB} = 1 - \left(\frac{\sum_i^{N_{modes}} \lambda_i^A + \lambda_i^B - \sum_i^{N_{modes}} \sum_j^{N_{modes}} \sqrt{\lambda_i^A \lambda_j^B} \left(\vec{v}_i^A \cdot \vec{v}_j^B \right)^2}{\sum_i^{N_{modes}} \lambda_i^A + \lambda_i^B} \right)^{\frac{1}{2}}. \tag{3}$$

Later, Grossfield et al. applied the same criterion to a set of 26 separate 100 ns trajectories [72]. The results strongly suggested that 100 ns (which at the time was a very long trajectory) was clearly not long enough for the protein fluctuations to converge well. Indeed, the average covariance overlaps for pairs of trajectories, considering only transmembrane region of the protein, was about 0.4, roughly the same value found by Faraĺdo-Gomez et al. for trajectories an order of magnitude shorter [123]. Furthermore, even individual loops, which one might suspect would be easier to sample than a whole protein, did not appear converged, in large part because they have more complex free energy surfaces with more distinct conformers that make significant contributions to the underlying ensemble.

More recently, several groups have performed microsecond-scale simulations of rhodopsin [67,92] and B2AR [68,69], which currently represents the state of the art. However, qualitative analyses suggest that even these simulations do not produce particularly good statistical sampling. For example, when Romo et al. computed all-to-all RMSD maps—aligning each snapshot of the protein against all others and color coding according to the RMS deviation—for long trajectories for rhodopsin and B2AR a block-diagonal structure was readily apparent, demonstrating the existence of substates persisting on the time scale of 100 s of nanoseconds [68]. The absence of significant off-diagonal peaks indicated that as a rule each state was visited only once. A similar conclusion was suggested by plots of the trajectory projected onto the first three principal components. Although qualitative methods of this sort cannot demonstrate that the statistics are good, they are valuable as easy-to-apply checks that can tell when the statistics are not very good. In addition, Zuckerman and coworkers applied one of their more sophisticated methods to the same rhodopsin data; they performed a simple clustering procedure

and created a hierarchy of states based on estimates of the interconversion rate between states [119]. This in turn allows them to directly assess the slower rates in the system, elegantly focusing on the large-scale motions that directly control all other observables. We believe that these assessments (both qualitative and quantitative) should become a standard part of every simulation project, because a careful analysis of the literature suggests an ongoing pattern of undue optimism with respect to statistical sampling. Implementations of all of these convergence assessment methods (and many other analysis tools) are released as part of LOOS, an open source library of tools for analyzing molecular dynamics simulations [126,127].

In contrast, it is often possible to apply far simpler models that are not plagued by convergence problems. For example, network models, which replace the complexity of all-atom force fields with harmonic springs connecting neighboring atoms, have been successfully applied to many protein systems [128,129], including GPCRs [130,131].

A recent paper shows that a well-tuned network model calculation represents protein fluctuations as well as one would expect from an MD simulation run for several hundred nanoseconds [74]. Given the enormous difference in their computational cost 1–2 min on a laptop for a network model versus weeks or months on a supercomputer for the MD, these are models that clearly should be considered carefully when designing computational projects.

6. Conclusions

Ever since the first high-resolution structure of rhodopsin was solved roughly 10 years ago, many groups have performed molecular dynamics simulations designed to explore the structure, fluctuations, and function of GPCRs. This number has increased dramatically in the last few years, with the publication of several new structures and significant increases in computational performance. As a result, many of the longest simulations ever run have been performed on GPCRs in the last few years. We have shown that simulations have made significant contributions in a number of areas, including protein–lipid interactions, internal protein hydration, and the conformational changes undergone during activation. In particular, close collaboration between simulation and experiment (particular solid state NMR) has proved to be exceptionally fruitful in generating exciting new insights into GPCR function.

Acknowledgments

References

[1] K. Lundstrom, Latest development in drug discovery on G protein-coupled receptors, Curr. Protein Pept. Sci. 7 (2006) 465–470.
[2] J.P. Overington, B. Al-Lazikani, A.L. Hopkins, How many drug targets are there? Nat. Rev. Drug Discov. 5 (2006) 993–996.
[3] R. Heilker, M. Wolff, C.S. Tautermann, M. Bieler, G-protein-coupled receptor-focused drug discovery using a target class platform approach, Drug Discov. Today 14 (2009) 231–240.
[4] K. Palczewski, T. Kumasaka, T. Hori, C.A. Behnke, H. Motoshima, B.J. Fox, Trong Le, D.C. Teller, T. Okada, R.E. Stenkamp, M. Yamamoto, M. Miyano, Crystal structure of rhodopsin: a G protein-coupled receptor, Science 289 (2000) 739–745.
[5] T. Okada, Y. Fujiyoshi, M. Silow, J. Navarro, E.M. Landau, Y. Shichida, Functional role of internal water molecules in rhodopsin revealed by X-ray crystallography, Proc. Natl Acad. Sci. U.S.A. 99 (2002) 5982–5987.
[6] P.C. Edwards, J. Li, M. Burghammer, J.H. McDowell, C. Villa, P.A. Hargrave, G.F.X. Schertler, Crystals of native and modified bovine rhodopsins and their heavy atom derivatives, J. Mol. Biol. 343 (2004) 1439–1450.
[7] J. Li, P.C. Edwards, M. Burghammer, C. Villa, G.F.X. Schertler, Structure of bovine rhodopsin in a trigonal crystal form, J. Mol. Biol. 343 (2004) 1409–1438.
[8] T. Okada, M. Sugihara, A.N. Bondar, M. Elstner, P. Entel, V. Buss, The retinal conformation and its environment in rhodopsin in light of a new 2.2 angstrom crystal structure. J. Mol. Biol. 342 (2004) 571–583.
[9] V. Cherezov, D.M. Rosenbaum, M.A. Hanson, S.G.F. Rasmussen, F.S. Thian, T.S. Kobilka, H.-J. Choi, P. Kuhn, W.I. Weis, B.K. Kobilka, R.C. Stevens, High-resolution crystal structure of an engineered human beta2-adrenergic G protein- coupled receptor, Science 318 (2007) 1258–1265.
[10] D.M. Rosenbaum, V. Cherezov, M.A. Hanson, S.G.F. Rasmussen, F.S. Thian, T.S. Kobilka, H.-J. Choi, X.-J. Yao, W.I. Weis, R.C. Stevens, B.K. Kobilka, GPCR engineering yields high-resolution structural insights into beta2- adrenergic receptor function, Science 318 (2007) 1266–1273.
[11] S.G.F. Rasmussen, H.-J. Choi, D.M. Rosenbaum, T.S. Kobilka, F.S. Thian, P.C. Edwards, M. Burghammer, V.R.P. Ratnala, R. Sanishvili, R.F. Fischetti, G.F.X. Schertler, W.I. Weis, B.K. Kobilka, Crystal structure of the human beta2 adrenergic g-protein-coupled receptor, Nature 450 (2007) 383–387.
[12] V.-P. Jaakola, M.T. Griffith, M.A. Hanson, V. Cherezov, E.Y.T. Chien, J.R. Lane, A.P. IJzerman, R.C. Stevens, The 2.6 angstrom crystal structure of a human A2A adenosine receptor bound to an antagonist, Science 322 (2008) 1211–1217.
[13] T. Warne, M.J. Serrano-Vega, J.G. Baker, R. Moukhametzianov, P.C. Edwards, R. Henderson, A.G.W. Leslie, C.G. Tate, G.F.X. Schertler, Structure of a beta1-adrenergic G-protein-coupled receptor, Nature 454 (2008) 486–491.
[14] P. Scheerer, J.H. Park, P.W. Hildebrand, Y.J. Kim, N. Krauss, H.-W. Choe, K.P. Hofmann, O.P. Ernst, Crystal structure of opsin in its G-protein-interacting conformation, Nature 455 (2008) 497–502.
[15] J.H. Park, P. Scheerer, K.P. Hofmann, H.-W. Choe, O.P. Ernst, Crystal structure of the ligand-free G-protein-coupled receptor opsin, Nature 454 (2008) 183–187.
[16] D. Salom, D.T. Lodowski, R.E. Stenkamp, I.L. Trong, M. Golczak, B. Jastrzebska, T. Harris, J.A. Ballesteros, K. Palczewski, Crystal structure of a photoactivated deprotonated intermediate of rhodopsin, Proc. Natl Acad. Sci. U.S.A. 103 (2006) 16123–16128.
[17] E.Y.T. Chien, W. Liu, Q. Zhao, V. Katritch, G.W. Han, M.A. Hanson, L. Shi, A.H. Newman, J.A. Javitch, V. Cherezov, R.C. Stevens, Structure of the human dopamine d3 receptor in complex with a d2/d3 selective antagonist, Science 330 (2010) 1091–1095.
[18] B. Wu, E.Y.T. Chien, C.D. Mol, G. Fenalti, W. Liu, V. Katritch, R. Abagyan, A. Brooun, P. Wells, F.C. Bi, D.J. Hamel, P. Kuhn, T.M. Handel, V. Cherezov, R.C. Stevens, Structures of the cxcr4 chemokine gpcr with small-molecule and cyclic peptide antagonists, Science 330 (2010) 1066–1071.
[19] B.K. Kobilka, X. Deupi, Conformational complexity of G-protein-coupled receptors, Trends Pharmacol. Sci. 28 (2007) 397–406.
[20] B. Kobilka, G.F.X. Schertler, New G-protein-coupled receptor crystal structures: insights and limitations, Trends Pharmacol. Sci. 29 (2008) 79–83.
[21] S. Topiol, M. Sabio, X-ray structure breakthroughs in the GPCR transmembrane region, Biochem. Pharmacol. 78 (2009) 11–20.
[22] F. Fanelli, P.G. De Benedetti, Computational modeling approaches to structure-function analysis of G protein-coupled receptors, Chem. Rev. 105 (2005) 3297–3351.
[23] B. Alberts, D. Bray, J. Lewis, M. Raff, K. Roberts, J.D. Watson, Molecular Biology of the Cell, third editionGarland Publishing, Inc, New York, 1994.
[24] J.A. Ballesteros, H. Weinstein, Analysis and refinement of criteria for predicting the structure and relative orientations of transmembranal helical domains, Biophys. J. 62 (1992) 107–109.
[25] G. Wald, A.B. Clark, Visual adaptation and chemistry of the rods, J. Gen. Physiol. 21 (1937) 93–105.
[26] F. Boll, Arch. Anat. Physiol. Physiol. Abstr. 4 (1877) 4–35.
[27] W.L. Hubbell, C. Altenbach, C.M. Hubbell, H.G. Khorana, Rhodopsin structure, dynamics, and activation: a perspective from crystallography, site-directed spin labeling, sulfhydryl reactivity, and disulfide cross-linking, Adv. Protein Chem. 63 (2003) 243–290.
[28] T.P. Sakmar, S.T. Menon, E.P. Marin, E.S. Awad, Rhodopsin: insights from recent structural studies, Annu. Rev. Biophys. Biomol. Struct. 31 (2002) 443–484.
[29] P.A. Baldwin, W.L. Hubbell, Effects of lipid environment on the light-induced conformational changes of rhodopsin: 2. Roles of lipid chain length, unsaturation, and phase state, Biochemistry 24 (1985) 2633–2639.
[30] N.J. Gibson, M.F. Brown, Lipid headgroup and acyl chain composition modulate the MI-MII equilibrium of rhodopsin in recombinant membranes, Biochem. 32 (1993) 2438–2454.
[31] M.F. Brown, Modulation of rhodopsin function by properties of the membrane bilayer, Chem. Phys. Lipids 73 (1994) 159–180.
[32] M.F. Brown, Influence of non-lamellar-forming lipids on rhodopsin, Curr. Top. Membr. 44 (1997) 285–356.
[33] M.F. Brown, Influence of nonlamellar-forming lipids on rhodopsin, Lipid polymorphism and membrane, Current Topics In Membranes, 44, 1997, pp. 285–356.
[34] K. Boesze-Battaglia, A.D. Albert, Fatty acid composition of bovine rod outer segment plasma membrane, Exp. Eye Res. 49 (1989) 699–701.
[35] W.L. Stone, C.C. Farnsworth, E.A. Dratz, A reinvestigation of the fatty acid content of bovine, rat and frog retinal outer segments, Exp. Eye Res. 28 (1979) 387–397.
[36] K. Boesze-Battaglia, T. Hennessey, A.D. Albert, Cholesterol heterogeneity in bovine rod outer segment disk membranes, J. Biol. Chem. 264 (1989) 8151–8155.
[37] S.E. Feller, K. Gawrisch, Properties of docosahexaenoic acid-containing lipids and their influence on the function of the GPCR rhodopsin, Curr. Opin. Struct. Bio. 15 (2005) 416–422.
[38] S.E. Feller, K. Gawrisch, T.B. Woolf, Rhodopsin exhibits a preference for solvation by polyunsaturated docosohexaenoic acid, J. Am. Chem. Soc. 125 (2003) 4434–4435.
[39] M.C. Pitman, A. Grossfield, F. Suits, S.E. Feller, Role of cholesterol and polyunsaturated chains in lipid–protein interactions: molecular dynamics simulation of

rhodopsin in a realistic membrane environment, J. Am. Chem. Soc. 127 (2005) 4576–4577.

[40] A. Grossfield, S.E. Feller, M.C. Pitman, A role for direct interactions in the modulation of rhodopsin by omega-3 polyunsaturated lipids, Proc. Natl Acad. Sci. U.S.A. 103 (2006) 4888–4893.

[41] O. Soubias, K. Gawrisch, Probing specific lipid–protein interaction by saturation transfer difference NMR spectroscopy, J. Am. Chem. Soc. 127 (2005) 13110–13111.

[42] A. Grossfield, S.E. Feller, M.C. Pitman, Contribution of omega-3 fatty acids to the thermodynamics of membrane protein solvation, J. Phys. Chem. B 110 (2006) 8907–8909.

[43] G. Khelashvili, A. Grossfield, S.E. Feller, M.C. Pitman, H. Weinstein, Structural and dynamic effects of cholesterol at preferred sites of interaction with rhodopsin identified from microsecond length molecular dynamics simulations, Proteins 76 (2009) 403–417.

[44] I.D. Alves, G.F.J. Salgado, Z. Salamon, M.F. Brown, G. Tollin, V.J. Hruby, Phosphatidylethanolamine enhances rhodopsin photoactivation and transducin binding in a solid supported lipid bilayer as determined using plasmon-waveguide resonance spectroscopy, Biophys. J. 88 (2005) 198–210.

[45] O. Soubias, S.-L. Niu, D.C. Mitchell, K. Gawrisch, Lipid-rhodopsin hydrophobic mismatch alters rhodopsin helical content, J. Am. Chem. Soc. (2008).

[46] P. H. Reggio, Drug addiction: from basic research to therapy, Springer, pp. 41–68.

[47] B. Jastrzebska, T. Maeda, L. Zhu, D. Fotiadis, S. Filipek, A. Engel, R.E. Stenkamp, K. Palczewski, Functional characterization of rhodopsin monomers and dimers in detergents, J. Biol. Chem. 279 (2004) 54663–54675.

[48] P. Kota, P.J. Reeves, U.L. Rajbhandary, H.G. Khorana, Opsin is present as dimers in COS1 cells: identification of amino acids at the dimeric interface, Proc. Natl Acad. Sci. U.S.A. 103 (2006) 3054–3059.

[49] S.E. Mansoor, K. Palczewski, D.L. Farrens, Rhodopsin self-associates in asolectin liposomes, Proc. Natl Acad. Sci. U.S.A. 103 (2006) 3060–3065.

[50] M. Chabre, R. Cone, H. Saibil, Is rhodopsin dimeric in native retinal rods? Nature 426 (2003) 30–31.

[51] D. Fotiadis, Y. Liang, S. Filipek, D.A. Saperstein, A. Engel, K. Palczewski, Rhodopsin dimers in native disc membranes, Nature 421 (2003) 127–128.

[52] D. Fotiadis, Y. Liang, S. Filipek, D.A. Saperstein, A. Engel, K. Palczewski, Is rhodopsin dimeric in native retinal rods? (reply), Nature 426 (2003) 31.

[53] S. Filipek, Organization of rhodopsin molecules in native membranes of rod cells–an old theoretical model compared with new experimental data, J. Mol. Model Online 11 (2005) 385–391.

[54] M. Filizola, H. Weinstein, The study of G-protein coupled receptor oligomerization with computational modeling and bioinformatics, FEBS J. 272 (2005) 2926–2938.

[55] M. Filizola, O. Olmea, H. Weinstein, Prediction of heterodimerization interfaces of G-protein coupled receptors with a new subtractive correlated mutation method, Protein Eng. 15 (2002) 881–885.

[56] X. Periole, T. Huber, S.-J. Marrink, T.P. Sakmar, G protein-coupled receptors self-assemble in dynamics simulations of model bilayers, J. Am. Chem. Soc. 129 (2007) 10126–10132.

[57] A.V. Botelho, T. Huber, T.P. Sakmar, M.F. Brown, Curvature and hydrophobic forces drive oligomerization and modulate activity of rhodopsin in membranes, Biophys. J. 91 (2006) 4464–4477.

[58] N.W. Downer, Cross-linking of dark-adapted frog photoreceptor disk membranes. evidence for monomeric rhodopsin. Biophys. J. 47 (1985) 285–293.

[59] R.A. Cone, Rotational diffusion of rhodopsin in the visual receptor membrane, Nat. New Biol. 236 (1972) 39–43.

[60] T.C. Edrington, M. Bennett, A.D. Albert, Calorimetric studies of bovine rod outer segment disk membranes support a monomeric unit for both rhodopsin and opsin, Biophys. J. 95 (2008) 2859–2866.

[61] M. Chabre, M. le Maire, Monomeric G-protein-coupled receptor as a functional unit, Biochemistry 44 (2005) 9395–9403.

[62] T.H. Bayburt, A.J. Leitz, G. Xie, D.D. Oprian, S.G. Sligar, Transducin activation by nanoscale lipid bilayers containing one and two rhodopsins, J. Biol. Chem. 282 (2007) 14875–14881.

[63] O.P. Ernst, V. Gramse, M. Kolbe, K.P. Hofmann, M. Heck, Monomeric gprotein-coupled receptor rhodopsin in solution activates its g protein transducin at the diffusion limit, Proc. Natl Acad. Sci. U.S.A. 104 (2007) 10859–10864.

[64] S. Banerjee, T. Huber, T.P. Sakmar, Rapid incorporation of functional rhodopsin into nanoscale apolipoprotein bound bilayer (nabb) particles, J. Mol. Biol. 377 (2008) 1067–1081.

[65] M.R. Whorton, M.P. Bokoch, S.G.F. Rasmussen, B. Huang, R.N. Zare, B. Kobilka, R.K. Sunahara, A monomeric g protein-coupled receptor isolated in a high-density lipoprotein particle efficiently activates its g protein, Proc. Natl Acad. Sci. U.S.A. 104 (2007) 7682–7687.

[66] M.R. Whorton, B. Jastrzebska, P.S.-H. Park, D. Fotiadis, A. Engel, K. Palczewski, R.K. Sunahara, Efficient coupling of transducin to monomeric rhodopsin in a phospholipid bilayer, J. Biol. Chem. 283 (2008) 4387–4394.

[67] A. Grossfield, M.C. Pitman, S.E. Feller, O. Soubias, K. Gawrisch, Internal hydration increases during activation of the G-protein-coupled receptor rhodopsin, J. Mol. Biol. 381 (2008) 478–486.

[68] T.D. Romo, A. Grossfield, M.C. Pitman, Concerted interconversion between ionic lock substates of the beta(2) adrenergic receptor revealed by microsecond timescale molecular dynamics, Biophys. J. 98 (2010) 76–84.

[69] R.O. Dror, D.H. Arlow, D.W. Borhani, M.Ø. Jensen, S. Piana, D.E. Shaw, Identification of two distinct inactive conformations of the beta2-adrenergic receptor reconciles structural and biochemical observations, Proc. Natl Acad. Sci. U.S.A. 106 (2009) 4689–4694.

[70] J.L. Klepeis, K. Lindorff-Larsen, R.O. Dror, D.E. Shaw, Long-timescale molecular dynamics simulations of protein structure and function, Curr. Opin. Struct. Biol. 19 (2009) 120–127.

[71] E. Lyman, C. Higgs, B. Kim, D. Lupyan, J.C. Shelley, R. Farid, G.A. Voth, A role for a specific cholesterol interaction in stabilizing the apo configuration of the human A(2A) adenosine receptor, Structure 17 (2009) 1660–1668.

[72] A. Grossfield, S.E. Feller, M.C. Pitman, Convergence of molecular dynamics simulations of membrane proteins, Proteins 67 (2007) 31–40.

[73] A. Grossfield, D.M. Zuckerman, Quantifying uncertainty and sampling quality in biomolecular simulations, Annu. Rep. Comput. Chem. 5 (2009) 23–48.

[74] T.D. Romo, A. Grossfield, Validating and improving elastic network models with molecular dynamics simulations, Proteins 79 (2011) 23–34.

[75] M. Filizola, H. Weinstein, Structural models for dimerization of G-protein coupled receptors: the opioid receptor homodimers, Biopolymers 66 (2002) 317–325.

[76] W. Guo, L. Shi, M. Filizola, H. Weinstein, J.A. Javitch, Crosstalk in G protein-coupled receptors: changes at the transmembrane homodimer interface determine activation, Proc. Natl Acad. Sci. U.S.A. 102 (2005) 17495–17500.

[77] M. Filizola, S.X. Wang, H. Weinstein, Dynamic models of G-protein coupled receptor dimers: indications of asymmetry in the rhodopsin dimer from molecular dynamics simulations in a popc bilayer, J. Comput. Aided Mol. Des. 20 (2006) 405–416.

[78] A. Bruno, A.E. Guadix, G. Costantino, Molecular dynamics simulation of the heterodimeric mGluR2/5HT2A complex. an atomistic resolution study of a potential new target in psychiatric conditions, J. Chem. Inf. Model. 49 (2009) 1602–1616.

[79] P.S.-H. Park, D.T. Lodowski, K. Palczewski, Activation of G protein-coupled receptors: beyond two-state models and tertiary conformational changes, Annu. Rev. Pharmacol. Toxicol. 48 (2008) 107–141.

[80] J. Saam, E. Tajkhorshid, S. Hayashi, K. Schulten, Molecular dynamics investigation of primary photoinduced events in the activation of rhodopsin, Biophys. J. 83 (2002) 3097–3112.

[81] B. Borhan, M.L. Souto, H. Imai, Y. Shichida, K. Nakanishi, Movement of retinal along the visual transduction path, Science 288 (2000) 2209–2212.

[82] V. Lemaître, P. Yeagle, A. Watts, Molecular dynamics simulations of retinal in rhodopsin: from the dark-adapted state towards lumirhodopsin, Biochemistry 44 (2005) 12667–12680.

[83] P.S. Crozier, M.J. Stevens, T.B. Woolf, How a small change in retinal leads to G-protein activation: initial events suggested by molecular dynamics calculations, Proteins: Struct., Funct., Bioinf. 66 (2007) 559–574.

[84] V. Hornak, S. Ahuja, M. Eilers, J.A. Goncalves, M. Sheves, P.J. Reeves, S.O. Smith, Light activation of rhodopsin: insights from molecular dynamics simulations guided by solid-state nmr distance restraints, J. Mol. Biol. 396 (2010) 510–527.

[85] E.C.Y. Yan, M.A. Kazmi, Z. Ganim, J.-M. Hou, D. Pan, B.S.W. Chang, T.P. Sakmar, R.A. Mathies, Retinal counterion switch in the photoactivation of the G protein-coupled receptor rhodopsin, Proc. Natl Acad. Sci. U.S.A. 100 (2003) 9262–9267.

[86] S. Lüdeke, M. Beck, E.C.Y. Yan, T.P. Sakmar, F. Siebert, R. Vogel, The role of glu181 in the photoactivation of rhodopsin, J. Mol. Biol. 353 (2005) 345–356.

[87] U.F. Röhrig, L. Guidoni, U. Rothlisberger, Early steps of the intramolecular signal transduction in rhodopsin explored by molecular dynamics simulations, Biochemistry 41 (2002) 10799–10809.

[88] U.F. Röhrig, L. Guidoni, A. Laio, I. Frank, U. Rothlisberger, A molecular spring for vision, J. Am. Chem. Soc. 126 (2004) 15328–15329.

[89] U.F. Röhrig, D. Sebastiani, Nmr chemical shifts of the rhodopsin chromophore in the dark state and in bathorhodopsin: a hybrid qm/mm molecular dynamics study, J. Phys. Chem. B 112 (2008) 1267–1274.

[90] F. Allen, G. Almasi, W. Andreoni, D. Beece, B.J. Berne, A. Bright, J. Brunheroto, C. Cascaval, J. Castanos, P. Coteus, P. Crumley, A. Curioni, M. Denneau, W. Donath, M. Eleftheriou, B. Fitch, B. Fleisher, C.J. Georgiou, R. Germain, M. Giampapa, D. Gresh, M. Gupta, R. Haring, H. Ho, P. Hochschild, S. Hummel, T. Jonas, D. Lieber, G. Martyna, K. Maturu, J. Moreira, D. Newns, M. Newton, R. Philhower, T. Picunko, J. Pitera, M. Pitman, R. Rand, A. Royyuru, V. Salapura, A. Sanomiya, R. Shah, Y. Sham, S. Singh, M. Snir, F. Suits, R. Swetz, W.C. Swope, N. Vishnumurthy, T.J.C. Ward, H. Warren, R. Zhou, Blue Gene: A vision for protein science using a petaflop supercomputer, IBM Syst. J. 40 (2001) 310.

[91] B.G. Fitch, R.S. Germain, M. Mendell, J. Pitera, M. Pitman, A. Rayshubskiy, Y. Sham, F. Suits, W.C. Swope, T.J.C. Ward, Y. Zhestkov, R. Zhou, Blue Matter, an application framework for molecular simulation on Blue Gene, J. Para. Distrib. Comp. 63 (2003) 759–773.

[92] K. Martínez-Mayorga, M.C. Pitman, A. Grossfield, S.E. Feller, M.F. Brown, Retinal counterion switch mechanism in vision evaluated by molecular simulations, J. Am. Chem. Soc. 128 (2006) 16502–16503.

[93] G.F.J. Salgado, A.V. Struts, K. Tanaka, S. Krane, K. Nakanishi, M.F. Brown, Solid-state 2 H NMR structure of retinal in metarhodopsini, J. Am. Chem. Soc. 128 (2006) 11067–11071.

[94] M.F. Brown, M.P. Heyn, C. Job, S. Kim, S. Moltke, K. Nakanishi, A.A. Nevzorov, A.V. Struts, G.F.J. Salgado, I. Wallat, Solid-state 2H NMR spectroscopy of retinal proteins in aligned membranes, Biochim. Biophys. Acta 1768 (2007) 2979–3000.

[95] A.A. Nevzorov, S. Moltke, M.P. Heyn, M.F. Brown, Solid-state NMR line shapes of uniaxially oriented immobile systems, J. Am. Chem. Soc. 121 (1999) 7636–7643.

[96] P.-W. Lau, A. Grossfield, S.E. Feller, M.C. Pitman, M.F. Brown, Dynamic structure of retinylidene ligand of rhodopsin probed by molecular simulations, J. Mol. Biol. 372 (2007) 906–917.

A. Grossfield / Biochimica et Biophysica Acta 1808 (2011) 1868–1878

[97] D.P. Hurst, A. Grossfield, D.L. Lynch, S. Feller, T.D. Romo, K. Gawrisch, M.C. Pitman, P.H. Reggio, A lipid pathway for ligand binding is necessary for a cannabinoid G protein-coupled receptor, J. Biol. Chem. 285 (2010) 17954–17964.

[98] D.C. Mitchell, B.J. Litman, Effect of ethanol on metarhodopsin II formation is potentiated by phospholipid polyunsaturation, Biochemistry 33 (1994) 12752–12756.

[99] D.C. Mitchell, J.T. Lawrence, B.J. Litman, Primary alcohols modulate the activation of the G protein-coupled receptor rhodopsin by a lipid-mediated mechanism, J. Biol. Chem. 271 (1996) 19033–19036.

[100] D.C. Mitchell, B.J. Litman, Effect of protein hydration on receptor conformation: decreased levels of bound water promote metarhodopsin II formation, Biochemistry 38 (1999) 7617–7623.

[101] D.C. Mitchell, B.J. Litman, Effect of ethanol and osmotic stress on receptor conformation. reduced water activity amplifies the effect of ethanol on metarhodopsin II formation. J. Biol. Chem. 275 (2000) 5355–5360.

[102] L. Pardo, X. Deupi, N. Dölker, M.L. López-Rodríguez, M. Campillo, The role of internal water molecules in the structure and function of the rhodopsin family of G protein-coupled receptors, Chembiochem 8 (2006) 19–24.

[103] T.E. Angel, M.R. Chance, K. Palczewski, Conserved waters mediate structural and functional activation of family a (rhodopsin-like) G protein-coupled receptors, Proc. Natl Acad. Sci. U.S.A. 106 (2009) 8555–8560.

[104] T.E. Angel, S. Gupta, B. Jastrzebska, K. Palczewski, M.R. Chance, Structural waters define a functional channel mediating activation of the GPCR, rhodopsin, Proc. Natl. Acad. Sci. USA 106 (2009) 14367–14372.

[105] T. Orban, S. Gupta, K. Palczewski, M.R. Chance, Visualizing water molecules in transmembrane proteins using radiolytic labeling methods, Biochemistry 49 (2010) 827–834.

[106] K. Gawrisch, personal, communication, 2011.

[107] E. Jardó n-Valadez, A.-N. Bondar, D.J. Tobias, Dynamics of the internal water molecules in squid rhodopsin, Biophy. J. 96 (2009) 2572–2576.

[108] K. Kaszuba, T. Róg, K. Bryl, I. Vattulainen, M. Karttunen, Molecular dynamics simulations reveal fundamental role of water as factor determining affinity of binding of β-blocker nebivolol to β₂-adrenergic receptor, J. Phys. Chem. B 114 (2010) 8374–8386.

[109] R. Baron, P. Setny, J.A. McCammon, Water in cavity-ligand recognition, J. Am. Chem. Soc. 132 (2010) 12091–12097.

[110] F. Raimondi, M. Seeber, P.G. De Benedetti, F. Fanelli, Mechanisms of inter- and intramolecular communication in gpcrs and g proteins, J. Am. Chem. Soc. 130 (2008) 4310–4325.

[111] N.G. Sgourakis, A.E. Garcia, The membrane complex between transducin and dark-state rhodopsin exhibits large-amplitude interface dynamics on the sub-microsecond timescale: Insights from all-atom md simulations, J. Mol. Biol. 398 (2010) 161–173.

[112] F. Fanelli, D. Dell'Orco, Rhodopsin activation follows precoupling with transducin: inferences from computational analysis, Biochemistry 44 (2005) 14695–14700.

[113] D. Dell'Orco, M. Seeber, F. Fanelli, Monomeric dark rhodopsin holds the molecular determinants for transducin recognition: insights from computational analysis, FEBS Lett 5 581 (2007) 944–948.

[114] T. Huber, S. Menon, T.P. Sakmar, Structural basis for ligand binding and specificity in adrenergic receptors: Implications for GPCR-targeted drug discovery, Biochemistry 47 (2008) 11013–11023.

[115] S. Vanni, M. Neri, I. Tavernelli, U. Rothlisberger, Observation of "ionic lock" formation in molecular dynamics simulations of wild-type beta 1 and beta 2 adrenergic receptors, Biochemistry 48 (2009) 4789–4797.

[116] J.A. Ballesteros, A.D. Jensen, G. Liapakis, S.G. Rasmussen, L. Shi, U. Gether, J.A. Javitch, Activation of the beta 2-adrenergic receptor involves disruption of an ionic lock between the cytoplasmic ends of transmembrane segments 3 and 6, J. Biol. Chem. 276 (2001) 29171–29177.

[117] D.A. Shapiro, K. Kristiansen, D.M. Weiner, W.K. Kroeze, B.L. Roth, Evidence for a model of agonist-induced activation of 5-hydroxytryptamine 2A serotonin receptors that involves the disruption of a strong ionic interaction between helices 3 and 6, J. Biol. Chem. 277 (2002) 11441–11449.

[118] W.F. van Gunsteren, J. Dolenc, Biomolecular simulation: historical picture and future perspectives, Biochem. Soc. Trans. 36 (2008) 11–15.

[119] X. Zhang, D. Bhatt, D.M. Zuckerman, Automated sampling assessment for molecular simulations using the effective sample size, J. Chem. Theory Comput. 6 (2010) 3048–3057.

[120] D.P. Hurst, A. Grossfield, D.L. Lynch, S. Feller, T.D. Romo, K. Gawrisch, M.C. Pitman, P.H. Reggio, A lipid pathway for ligand binding is necessary for a cannabinoid G protein-coupled receptor, J. Biol. Chem. (2010).

[121] H. Flyvbjerg, H.G. Petersen, Error estimates on averages of correlated data, J. Chem. Phys. 91 (1989) 461–466.

[122] B.A. Berg, R. Harris, From data to probability density without histograms, Comp. Phys. Comm. 179 (2008) 443–448.

[123] J.D. Faráldo-Gomez, L.R. Forrest, M. Baaden, P.J. Bond, C. Domene, G. Patargias, J. Cutherbertson, M.S.P. Sansom, Conformational sampling and dynamics of membrane proteins from 10-nanosecond computer simulations, Proteins 57 (2004) 783–791.

[124] B. Hess, Similarities between principal components of protein dynamics and random diffusion, Phys. Rev. E 62 (2000) 8438–8448.

[125] B. Hess, Convergence of sampling in protein simulations, Phys. Rev. E 65 (2002), 031910-10.

[126] T.D. Romo, A. Grossfield, LOOS: an extensible platform for the structural analysis of simulations, Conf. Proc. IEEE Eng. Med. Biol. Soc. 2009 (2009) 2332–2335.

[127] T.D. Romo, A. Grossfield, LOOS: A lightweight object-oriented software library, http://loos.sourceforge.net. (2010).

[128] C. Chennubhotla, A.J. Rader, L.-W. Yang, I. Bahar, Elastic network models for understanding biomolecular machinery: from enzymes to supramolecular assemblies, Phys. Biol. 2 (2005) S173–S180.

[129] I. Bahar, T.R. Lezon, A. Bakan, I. Shrivastava, Normal mode analysis of biomolecular structures: functional mechanisms of membrane proteins, Chem. Rev. 110 (2010) 1463–1497.

[130] A.J. Rader, G. Anderson, B. Isin, H.G. Khorana, I. Bahar, J. Klein-Seetharam, Identification of core amino acids stabilizing rhodopsin, Proc. Nat. Acad. Sci. U.S.A. 101 (2004) 7246–7251.

[131] B. Isin, A.J. Rader, H.K. Dhiman, J. Klein-Seetharaman, I. Bahar, Predisposition of the dark state of rhodopsin to functional changes in structure, Proteins 65 (2006) 970–983.